Effects of long-term treatment with the dipeptidyl peptidase-4 inhibitor vildagliptin on endocrine cells in non-obese type 2 diabetic Goto-Kakizaki rats

（非肥満型２型糖尿病モデル後藤－柿崎ラットの膵内分泌細胞に対するジペプチジルペプチダーゼ４阻害薬ビルダグリプチンによる長期治療の効果）

申　請　者　　弘前大学大学院医学研究科
病態制御科学領域　病態病理学教育研究分野

氏　　名　　稲　葉　渉

指導教授　　水　上　浩　哉

Abstract

Reduced ß cell mass is a characteristic feature of type 2 diabetes and incretin therapy is expected to prevent this condition. However, it is unknown whether dipeptidyl peptidase-4 inhibitors influence ß and α cell mass in animal models of diabetes that can be translated to humans. Therefore, we examined the long-term effects of treatment with the dipeptidyl peptidase-4 inhibitor vildagliptin on islet morphology in Goto-Kakizaki (GK) rats, a spontaneous, non-obese model of type 2 diabetes, and explored the underlying mechanisms. Four-week-old GK rats were orally administered with vildagliptin (15 mg/kg) twice daily for 18 weeks. Glucose tolerance was monitored during the study. After 18 weeks, ß and α cell morphology and the expression of molecules involved in cell proliferation and cell death were examined by immunohistochemistry and morphometric analysis. We found that vildagliptin improved glucose tolerance and insulin secretion, and suppressed hyperglucagonemia by increasing plasma active glucagon-like peptide-1 concentrations. ß cell mass was reduced in GK rats to 40% of that in Wistar rats, but was restored to 80% by vildagliptin. Vildagliptin enhanced ß and α cell proliferation, and increased the number of small neogenetic islets. Vildagliptin also reduced the number of 8-hydroxy-2′-deoxyguanosine-positive cells and forkhead box protein O1 expression, inhibited macrophage infiltration, and enhanced S6 ribosomal protein, molecule of target of rapamycin, and pancreatic duodenal homeobox 1 expression. These results indicate that starting vildagliptin treatment from an early age improved glucose tolerance and preserved islet ß cell mass in GK rats by facilitating the proliferation of islet endocrine cells.

Keywords

Type 2 diabetes; Dipeptidyl peptidase-4 inhibitor; Glucagon-like peptide-1; ß cells; α cells; (GK rat)

1. Introduction

The emergence of incretin therapies, exemplified by glucagon-like peptide (GLP)-1 and dipeptidyl peptidase (DPP)-4 inhibitors, has drastically changed the direction of diabetes treatment. Studies within clinical practice have confirmed that incretin therapies suppress hyperglycemia by promoting insulin secretion in patients with type 2 diabetes (Bosi et al., 2008 and Nauck et al., 2009). However, there is no convincing proof showing that incretin therapies promote the regeneration of islet ß cells or protect against ß cell death in patients with diabetes.

Type 2 diabetes is characterized by insulin resistance and poor insulin secretion, which predominate in the obese and lean phenotypes, respectively (Funakoshi et al., 2008 and SEARCH for Diabetes in Youth Study Group). The response of islet ß cells to DPP-4 inhibitors may therefore vary among patients with type 2 diabetes. However, no studies have examined the possible differences in incretin effects between obese and lean patients with type 2 diabetes. To address this issue, studies using appropriate animal models may be useful to translate the findings to humans. Some reports have described beneficial effects of DPP-4 inhibitors on islet structures in obese animal models of type 2 diabetes, including Zucker diabetic fatty rats (Brand et al., 2009 and Sudre et al., 2002), db/db mice (Moritoh et al., 2010), high-fat diet-induced obese animals (Lamont and Drucker, 2008), and low-dose streptozotocin-induced diabetic mice (Mu et al., 2006). Unfortunately, information is lacking on the effects of DPP-4 inhibitors on non-obese diabetic animals. Similarly, their effects on other islet endocrine cells, especially α cells, have yet to be determined.

The Goto-Kakizaki (GK) rat is a non-obese animal model of type 2 diabetes characterized by low insulin secretion, similar to that in Asian patients with type 2 diabetes (Goto et al., 1988 and Portha et al., 1991). The islet pathology in this model involves a progressive decline of ß cell mass (Koyama et al., 1998 and Koyama et al., 2000). Only a few studies have addressed the effects of GLP-1 or exenatide on ß cell growth (Svensson et al., 2007 and Tourrel et al., 2002) and function in GK rats (Mukai et al., 2011 and Simonsen et al., 2009), but no studies have examined the effects of DPP-4 inhibitors in this model. Under these circumstances, we examined the effects of treatment with a DPP-4 inhibitor on islet morphology in GK rats. We also explored the mechanisms involved in the changes induced by the DPP-4 inhibitor.

2. Materials and methods

2.1. Rats, vildagliptin treatment, and tissue processing

Male GK and Wistar rats were purchased from CLEA Japan Inc. (Tokyo, Japan). Based on the blood levels of glucose and body weight, 4-week-old rats (about 1 week after weaning) were assigned into two balanced groups and were orally administered with the DPP-4 inhibitor vildagliptin (provided by Novartis, Basel, Switzerland) at a dose of 15 mg/kg twice daily (09:00 h and 18:00 h), or with vehicle alone (untreated group). The animals were fed a standard diet (CE-2, CLEA Japan) ad libitum. Wistar rats were used as a non-diabetic control and were treated with vildagliptin in the same way. The treatment was started at 4 weeks of age and was continued for 18 weeks to 22 weeks of age.

The dose of vildagliptin was set at 30 mg/kg/day because this dose was expected to enhance insulin secretion and β cell proliferation based on the results of previous studies (equivalent to 50 mg/kg twice daily in humans, or double the normal daily dose) (Burkey et al., 2005 and Duttaroy et al., 2011). During the study, we regularly measured the body weight and food intake of each rat. Rats underwent a 2 g/kg oral glucose tolerance test after an overnight fast at the start of the study, and after 8 and 18 weeks of treatment. At 18 weeks, we also measured plasma insulin levels before (i.e., fasting) and at 30 min after the glucose challenge. One day before sacrificing the rats, non-fasting blood glucose concentrations were measured at 11:00 h. At the end of the study, the rats were fasted overnight and then euthanized with an overdose of pentobarbital (Abbott Laboratories, Chicago, IL) injected intraperitoneally. Blood was withdrawn from right cardiac atrium for the measurement of glucose and lipids. The pancreas was harvested for biochemical and immunohistochemical analyses.

For structural and immunohistochemical evaluations, the pancreas was fixed in 4% formaldehyde. A portion of the pancreas was quickly frozen to measure insulin content. As a reference, the pancreas was also obtained from GK and Wistar rats at 4 weeks of age.

All of the procedures followed the 'Principles of Laboratory Animal Care' (National Institutes of Health publication no. 85–23, revised 1985) and the institutional guidelines of Hirosaki University Animal Experimentation for the care and use of laboratory animals (approval #M05032). Each group consisted of 6–9 rats.

2.2. Measurement of blood glucose, insulin, glucagon, GLP-1 and pancreatic insulin content

Blood glucose was measured in tail blood using a Glucose C-II test (Wako Pure Chemical Industries, Osaka, Japan). Insulin and glucagon concentrations were measured in plasma samples stored at −75 °C in heparinized tubes using enzyme-linked immunosorbent assay (ELISA) kits (insulin: Morinaga Biol. Sci., Yokohama, Japan; glucagon: Wako). To measure the active form of GLP-1, blood samples were collected in EDTA-coated tubes, mixed with 10 mg/ml vildagliptin, and centrifuged. Active GLP-1 was measured in the resulting plasma using an ELISA kit (Shibayagi Co., Ltd., Maebashi, Japan), as previously described (Burkey et al., 2005 and Duttaroy et al., 2011). Serum triglyceride and total cholesterol concentrations were measured using enzymatic colorimetric reagents (Triglyceride E-test and Cholesterol E-test, respectively; Wako), as previously described (Mizukami et al., 2012).

To measure pancreatic insulin content, the pancreatic tissues were homogenized in acid–ethanol solution and centrifuged at 15,000 rpm for 15 min at 4 °C. The insulin content in the supernatant was measured using an ELISA kit (Morinaga Biol. Sci., Yokohama, Japan).

2.3. Histological examination and immunohistochemistry

All of the fixed tissues were embedded in paraffin and stained with hematoxylin and eosin (H&E) for review. The β and α cells were identified by double-immunostaining with streptavidin–biotin (Nichirei Histofine®; Nichirei Co., Tokyo, Japan). Briefly, deparaffinized sections were first incubated with rabbit anti-glucagon antibody (Dako Cytomation, Glostrup, Denmark) for 1 h. Then, the slides were incubated with a biotinylated anti-rabbit immunoglobulin antibody and alkaline phosphatase-conjugated streptavidin for 30 min each. The alkaline phosphatase reaction was detected using a fuchsin staining kit (Nichirei). After rinsing, the sections were incubated with a polyclonal anti-insulin antibody (Dako) for 1 h. Sections were then incubated with biotinylated immunoglobulin and peroxidase-conjugated streptavidin. Finally, the reaction products were visualized with a diaminobenzidine staining kit (Dako). Nuclei were lightly counterstained with hematoxylin.

To evaluate oxidative stress-related cell damage and inflammatory status, sections were immunostained with monoclonal antibodies to 8-hydroxy-2′ -deoxyguanosine (8OHdG) (JICA, Nikken Seil Co., Ltd., Fukuroi, Japan), and Iba-1 (Wako) (a marker of

macrophage), respectively. The sections were then incubated with the secondary antibodies, biotinylated anti-mouse immunoglobulin antibody and peroxidase-conjugated streptavidin (Dako), for 30 min each, and the reaction products were colorized by diaminobenzidine (Dako). To objectively evaluate 8OHdG-positivity, we first set the background intensity of nuclei in acinar cells as 1.0 in densitometric analysis. We then measured the intensity of islet cell nuclei. Cells with a nuclear density >2 fold higher than that of acinar cells were defined as positive. We then determined the percentage of positive cells among 300–400 nuclei per rat. Iba-1 positive cells in the islet were quantified and expressed as the number per unit islet area in each rat.

To identify proliferating cells among the ß and α cells, we performed immunohistochemical double-staining of Ki-67 (Abcam, Cambridge, UK) and insulin or glucagon. The percentage of cells expressing Ki-67 (MIB 1 index) was determined by counting the number of clearly stained nuclei among 300–400 islet cells. Cells undergoing apoptosis were identified by terminal deoxynucleotidyl transferase dUTP nick end labeling (TUNEL) with an ApoTag® kit (Millipore, Bellerica, MA, USA). The presence or absence of apoptosis was confirmed by comparison with a positive control tissue (lymph node) containing apoptotic cells placed on the same slides. To explore whether the signals controlling the proliferation and apoptosis of ß cells were activated, we determined the immunohistochemical expression of pancreatic duodenal homeobox 1 (PDX-1; Epitomics, Burlingame, CA, USA), phospho-mTOR (molecule of target of rapamycin; p-mTOR; Ser2448; Cell Signaling Technology, Inc., Danvers, MA, USA), phospho-S6 ribosomal protein (Ser235/236; p-S6RP; Cell Signaling Technology), and forkhead box protein O1 (FoxO1; C29H4; Cell Signaling Technology) using the specified antibodies. Staining intensity was compared by placing four pancreatic tissues from each group on the same slide and applying the same staining conditions. The reactions were semiquantified for 20–30 islets as 0=negative, 1=weakly positive, 2=clearly positive against the negative background, and 3=strongly positive. The mean immunoreactive intensity was determined for each rat.

2.4. Morphometric analysis

Quantitative evaluation of the islet was performed using a computer-assisted point-counting method on an Olympus AX80 microscope (Olympus, Tokyo, Japan) connected to a personal computer system running NIH imageJ software (Version 1.56; NIH, Bethesda, MD, USA). The volume density of α and ß cells was calculated with the

point-counting method as previously described (Koyama et al., 1998 and Koyama et al., 2000). First, a low magnification view (×40) of H&E-stained sections of the whole pancreas was captured for each rat. The images were overlaid on a grid consisting of 450 points. Islet volume density was determined by dividing the total number of points on islet cells by the total number of points on the pancreatic parenchyma and mesenchymal tissues.

To quantify the numbers of ß and α cells, a high-magnification image (×200) of double-labeled sections was overlaid on a grid consisting of 875 points. The volume densities of ß and α cells were determined by dividing the total number of points on insulin- or glucagon-stained cells by the total number of points on the pancreatic parenchyma. The total ß and α cell masses were determined by multiplying the volume density by pancreas volume. The mean sizes of the ß and α cells were determined in individual animals by dividing the total cell area by the total number of nuclei counted. The mean cell sizes were then calculated for each group. The areas of blood vessels, nerves, fat, and connective tissues were excluded from these measurements.

2.5. Evaluation of neogenetic islets

Small clusters or isolated islet cells stained positive for insulin and glucagon were dispersed in the ductal, periductal, and acinar areas. Neogenetic islets were defined as individual insulin-positive cells or small aggregates of <4 endocrine cells (Paris et al., 2004). The number of neogenetic islets was counted and expressed as the number per unit area of the pancreas.

2.6. Statistical analysis

All immunohistochemical evaluations and morphometric analyses were conducted by investigators blinded to the treatment group. All values are expressed as means±S.E.M. Multiple groups were compared by nonparametric one way of analysis of variance, followed by Bonferroni/Dunn or Fisher's PLSD tests for multiple comparisons. Unpaired Mann–Whitney tests were used for comparisons between the vildagliptin-treated and untreated groups. Values of $P<0.05$ were considered to be statistically significant.

3. Results

3.1. Laboratory findings and food intake

From the start of the experiment, the body weight of GK rats at 4 weeks of age was 25% less than that of Wistar rats (Table 1). The GK rats at this age already showed marked hyperglycemia compared with Wistar rats, although there was no significant reduction in β cell volume density (Table 2). The difference in body weight between GK rats and Wistar rats remained constant throughout the study. Treatment with vildagliptin did not affect body weight of GK or Wistar rats. Fasting and non-fasting blood glucose levels were markedly higher in GK rats than in Wistar rats at the end of the experiment. Vildagliptin decreased blood glucose levels in GK rats but not in Wistar rats (Table 1). At end of the experiment, serum TG concentrations were decreased in untreated GK rats, and were unaffected by vildagliptin. Food intake adjusted for body weight at the end of the experiment was similar in both Wistar and GK rats (mean intake 6.8 g/day vs. 6.6 g/day). Vildagliptin did not influence food intake in Wistar rats (6.5 g/day), but did slightly but significantly reduce food intake in GK rats (mean change, 13.6%; 5.7 g/day; $P<0.05$ vs. untreated GK rats).

3.2. Glucose intolerance and insulin secretion

The temporal changes in glucose intolerance determined by the glucose tolerance test are shown in Fig. 1. At the start of the experiment, 4-week-old GK rats already showed post-challenge hyperglycemia. Vildagliptin suppressed post-challenge hyperglycemia to a similar extent at weeks 8 and 18 of treatment in GK rats, but did not affect post-challenge hyperglycemia in Wistar rats.

Fasting plasma insulin concentrations were not significantly different among the four experimental groups (Fig. 2A). Insulin secretion in response to the 2 g/kg glucose challenge was significantly decreased in untreated GK rats compared with Wistar rats. Vildagliptin increased glucose-stimulated insulin secretion in GK rats compared with that in untreated GK rats, but did not affect glucose-stimulated insulin secretion in Wistar rats.

3.3. Plasma glucagon and GLP-1 concentrations

At the end of the experiment, fasting plasma glucagon concentrations were increased in GK rats compared with Wistar rats, but were reduced to normal levels by

vildagliptin (Fig. 2B). There was a significant decrease in plasma GLP-1 concentrations in untreated GK rats, while vildagliptin increased GLP-1 concentrations in these rats.

3.4. Pancreatic insulin content

Pancreatic insulin content in GK rats was decreased to 28% of that in Wistar rats (Fig. 2C). Vildagliptin partially recovered insulin content in GK rats.

3.5. Islet morphometry

Islet volume density was reduced in GK rats compared with Wistar rats (Table 2). Treatment with vildagliptin increased islet volume density.

Double-labeling of insulin and glucagon revealed a mixed composition of islet endocrine cells, with the center of the islets mainly composed of ß cells and the periphery by α cells (Fig. 3A). Although the composition of islet endocrine cells was clear in GK rats, the specific distribution of ß and α cells was lost and irregular processes or budding of endocrine cells were found. The islets in vildagliptin-treated GK rats showed enlargement and expansion of ß cells.

At 4 weeks of age there was no significant difference in the volume densities of ß and α cells between Wistar and GK rats (Table 2). However, at the end of the experiment, the volume density of ß cells was reduced in GK rats compared with Wistar rats (Fig. 3B). Vildagliptin nearly normalized the volume density of ß cells in GK rats, but not in Wistar rats. Islet volume and ß cell volume were reduced in GK rats to less than half of that in Wistar rats, while vildagliptin restored these parameters to near those in Wistar rats (Table 2). The volume density of α cells in GK rats was similar to that in Wistar rats and vildagliptin did not influence this parameter (Fig. 3B). The sizes of ß or α cells were not different between GK and Wistar rats, and were not affected by vildagliptin (Table 2).

3.6. Apoptosis and proliferation of islet cells

Islet cells of GK and Wistar rats treated with or without vildagliptin were not apoptotic based on TUNEL staining, whereas lymph node and intestinal mucosa tissue sections, as positive controls included on the same slides, contained several apoptotic cells (Supplementary Fig. 1). Ki-67 staining demonstrated the proliferation of cells within and outside the islet, although infrequently (Fig. 4A). Double-labeling studies

confirmed that vildagliptin increased the proliferation rate of ß and α cells (Fig. 4B).

3.7. Expression of cell signaling molecules and 8OHdG

To examine the activity of downstream components of the GLP-1 signaling pathway, we conducted immunohistochemistry for the phosphorylated forms of PDX-1, mTOR, S6RP, and FoxO1. PDX-1 is a crucial transcription factor for ß cell differentiation and cell growth. mTOR and S6RP are molecules that promote cellular proliferation, while FoxO1 mediates apoptotic signals. Islet PDX-1 expression was markedly reduced in GK rats compared with Wistar rats (Fig. 5A). Vildagliptin restored PDX-1 expression in the islets of GK rats (Fig. 5B). The staining intensities of p-S6RP and p-mTOR were also reduced in the islets of GK rats compared with those in Wistar rats (Fig. 6A). The staining intensities of both proteins were improved in vildagliptin-treated GK rats. By contrast, the nuclear expression of FoxO1 was augmented in the islets of GK rats compared with that in Wistar rats, while vildagliptin suppressed its expression in GK rats. Semiquantitative evaluation confirmed these findings (Fig. 6B).

Nuclear expression of 8OHdG in islet cells was low in Wistar rats but was much greater in GK rats (Fig. 7A). Vildagliptin reduced the staining intensity of 8OHdG in GK rats. Semiquantitative evaluation confirmed these findings (Fig. 7B).

3.8. Identification of neogenetic islets

One of the robust changes in GK rats was the appearance of isolated or small clusters of endocrine cells (Fig. 8A). These cells were mainly found in the ductal, periductal, and acinar areas. Quantification of the isolated or small clusters of ß and α cells (<4 cells) demonstrated that the number of ß cell clusters was greater in GK rats than in Wistar rats, and was further increased in vildagliptin-treated GK rats (Fig. 8A). By contrast, α cell clusters were widely scattered in Wistar rats and less so in GK rats. Vildagliptin promoted the appearance of α cell clusters in GK rats.

3.9. Macrophage infiltration

The islets in GK rats showed extensive macrophage infiltration based on the intensity of Iba-1 staining (Fig. 9A). Quantification of Iba-1-positive cells demonstrated that macrophage infiltration was suppressed by vildagliptin (Fig. 9B).

4. Discussion

In the present study, long-term treatment with the DPP-4 inhibitor vildagliptin for 18 weeks from an early age improved glucose intolerance, promoted glucose-stimulated insulin secretion, and suppressed hyperglucagonemia in GK rats. Vildagliptin also enhanced the preservation of pancreatic insulin content, β cell volume, and β and α cell proliferation, and increased the number of small neogenetic islets. Previous studies have documented the expansion of β cell mass in 2-month-old GK rats treated with GLP-1 or exendin-4 at the age of 2–6 days (Tourrel et al., 2002). However, treatment with exendin-4 for 12 weeks in adult GK rats (10 weeks old) did not increase α and β cell volume densities compared with untreated rats, although only 4 islets were subjected to analysis in each rat in that group (Svensson et al., 2007). In the present study, long-term treatment with vildagliptin from 4 weeks of age preserved islet endocrine cells by increasing the proliferation of β and α cells in GK rats. The protective effects of vildagliptin on islet morphology and function in GK rats observed here are consistent with data obtained in other models of type 2 diabetes, including high-cholesterol diet-induced diabetic rats and human islet amyloid polypeptide-overexpressing rats (Cummings et al., 2010 and Matveyenko et al., 2009). Some novel findings of our study are that vildagliptin increased the number of small neogenetic islets and stimulated the proliferation of α cells.

The progressive decline of β cell mass is a salient feature of type 2 diabetes in humans (Sakuraba et al., 2002 and Butler et al., 2003). β cell mass is determined by the balance between cell death and proliferation. Although the reduction in β cell number in humans was proposed to be caused by increased apoptosis (Butler et al., 2003), apoptosis is not commonly detected in humans with non-obese type 2 diabetes (Sakuraba et al., 2002). There may be a difference in the temporal changes in β cell decline between obese and lean type 2 diabetes because the β cell mass in obese non-diabetic subjects was greater than that in lean non-diabetic subjects (Butler et al., 2003). The reduction in β cell mass in obese diabetic subjects was much greater than that in lean diabetic subjects (Butler et al., 2003). Obese type 2 diabetic animal models, such as db/db mice (Leiter et al., 1979) or Zucker diabetic fatty rats (Higa et al., 1999), exhibit temporal islet hyperplasia with a subsequent decline in β cell mass caused by β cell death. Unlike these animals, GK rats do not show evidence of islet hyperplasia (Koyama et al., 2000 and Svensson et al., 2007). Therefore, the results obtained using GK rats may be applicable to lean type 2 diabetes in humans. Indeed, several studies have shown an absence of apoptotic cells in mature GK rats (Koyama et al., 1998,

Koyama et al., 2000 and Mizukami et al., 2012). In the present study, we could not detect a meaningful number of apoptotic β or α cells in GK rats. Consequently, we cannot determine to what extent the protection against β cell apoptosis contributes to the maintenance of islets in vildagliptin-treated GK rats. Nevertheless, the decreased number of 8OHdG-positive cells and reduced FoxO1 expression in vildagliptin-treated GK rats suggest that vildagliptin activates potent defense mechanisms to prevent β cell death (Martinez et al., 2008) that cannot be identified by conventional TUNEL staining. Such findings appear to support a recent study showing that exenatide suppresses oxidative stress by inhibiting Src in GK rats (Mukai et al., 2011).

In addition to protecting against cell death, our studies indicate that the preservation of β cell mass may be achieved through increased proliferation of β cells, the growth of which is significantly impaired in young GK rats (Koyama et al., 1998). The increased number of Ki-67-positive cells together with the enhanced expression of cell proliferating signals (PDX-1, p-mTOR, and p-S6RP) that were detected in this study are consistent with the findings that β cell growth is stimulated by glucose, GLP-1, or exenatide in vitro (Kwon et al., 2004). Although other molecules, including phosphatidyl inositol-3 kinase and Akt, may also be involved in this process, we could not determine their expression because immunostaining for these signals was too weak (data not shown). Additional studies using fresh samples are needed to confirm the underlying molecular changes.

In patients with type 2 diabetes, hyperglucagonemia is known to contribute to uncontrolled hyperglycemia and could therefore represent an important treatment target (Dunning and Gerich, 2007 and Gromada et al., 2007). Treatment with DPP-4 inhibitors was reported to suppress hyperglucagonemia in patients with type 2 diabetes (Dunning et al., 2005 and Hare et al., 2010). Our finding that vildagliptin suppressed hyperglucagonemia may therefore be relevant for improving blood glucose control. The increased proliferation of α cells in vildagliptin-treated GK rats, as determined using Ki-67 and glucagon double-staining, was therefore surprising, although the total α cell mass was not significantly altered. Unlike our findings, reductions in α cell area and number in the islet were detected in streptozotocin-induced diabetic mice when treated with sitagliptin (Takeda et al., 2012). However, in that study, the rates of cell death or proliferation of α cells in sitagliptin-treated diabetic mice were not examined. It is unclear whether these discrepant results are due to differences between animal species, analytical methods, or DPP-4 inhibitors. Nevertheless, increased α cell proliferation is not necessarily detrimental for glucose tolerance, as it may enhance β cell function or replication through paracrine pathways by releasing GLP-1 or acetylcholine

(Ellingsgaard et al., 2011 and Rodriguez-Diaz et al., 2011). Alternatively, vildagliptin-induced ß cell activation may also contribute to α cell proliferation by releasing growth factors (Kawamori et al., 2011). Our preliminary studies on the expression of PC1/3 have so far been unsuccessful, so the implication of increased α cells is still unclear. Future studies should examine whether there are phenotypic changes in α cells favoring enhanced GLP-1 secretion.

An increase in foci consisting of small clusters of endocrine cells in vildagliptin-treated animals is particularly interesting, and these foci were referred to as small neogenetic islets in other reports (Paris et al., 2004 and Bonner-Weir et al., 2010). Newly produced ß cells may be derived from limited pathways, including replication from preexisting ß cells, differentiation of islet stem cells, primitive cells in the duct or progenitor cells scattered in acinar cell areas, or transdifferentiation from other exocrine components (Bonner-Weir et al., 2010). Although small neogenetic islets may contribute to an increase in total ß cell mass, it is likely that the preservation of ß cell mass was mainly achieved by the expansion of Ki-67-positive ß cells within pre-existing islets in vildagliptin-treated GK rats. Compared with Wistar rats, small neogenetic islets were scattered widely in GK rats and may be indicative of attempts to compensate for ß cell decline. Our findings suggest that vildagliptin may promote attempts to increase ß cell mass by increasing GLP-1 concentrations. In fact, the GLP-1 receptor was expressed in ductal cells and ß cells, and GLP-1 receptor-positive progenitor cells located in the duct and exocrine cells probably responded to the elevated GLP-1 concentrations (Bonner-Weir et al., 2010). It should be noted, however, that the expanded ß cells in vildagliptin-treated GK rats did not fully compensate for the reduced ß cell function because glucose tolerance was only partially recovered. This may be accounted for by immaturity or an innate incapacity of insulin secretion of newly derived ß cells in GK rats.

Anti-inflammatory activities of GLP-1 may also be involved in the improved islet pathology in vildagliptin-treated GK rats because inflammatory changes in the islets, including macrophage migration, are established features of this model (Homo-Delarche et al., 2006 and Ehses et al., 2009). In this study, we found that macrophage infiltration into islets was significantly reduced in vildagliptin-treated GK rats. Administration of an interleukin-1 antagonist to alter immunoregulation reduced the inflammatory changes in the islets and improved hyperglycemia in GK rats (Ehses et al., 2009). It is therefore conceivable that the increased blood GLP-1 concentrations in vildagliptin-treated GK rats may have protected against islet injury by suppressing inflammatory activity. In fact, exenatide was recently shown to protect against

inflammatory process of atherosclerotic lesions and renal injury in diabetic animals independent of hyperglycemia (Arakawa et al., 2010 and Kodera et al., 2011). In our study design, however, the mechanisms responsible for the improvements in islet structure are not fully clear because improved glucose intolerance, effects of circulating/local cytokines, and direct inhibition of DPP-4 expressed in the islet cells or in migrating cells may be involved. Nevertheless, in situ characterization of the effects of vildagliptin in GK rats may provide valuable information for the clinical application of vildagliptin to patients with type 2 diabetes.

Contribution statement

WI, HM, and SY conceived and designed the experiments, or analyzed and interpreted the data. SY drafted the article and revised it critically for intellectual content. All of the authors read and approved the final version of the manuscript to be published.

Acknowledgment

The authors thank Ms. Shiho Fujiwara, Mari Tsujii, Mrs. Saori Ogasawara, and Mrs. Hiroko Mori for their technical assistance. The study was partly supported by a Research Grant from Novartis. Some of this work was presented at the 46th Annual Meeting of the European Association for the Study of Diabetes in Stockholm, September 21–23, 2010.

References

1. Arakawa, M., Mita, T., Azuma, K., Ebato, C., Goto, H., Nomiyama, T., Fujitani, Y., Hirose, T., Kawamori, R., Watada, H. 2010. Inhibition of monocyte adhesion to endothelial cells and attenuation of atherosclerotic lesion by a glucagon-like peptide-1 receptor agonist, exendin-4. Diabetes 59, 1030-1037.

2. Bonner-Weir, S., Li, W.C., Ouziel-Yahalom, L., Guo, L., Weir, G.C., Sharma, A. 2010. Beta-cell growth and regeneration: replication is only part of the story. Diabetes 59, 2340-2348.

3. Bosi, E., Lucotti, P., Setola, E., Monti, L., Piatti, P.M. 2008. Incretin-based therapies in type 2 diabetes: a review of clinical results. Diabetes Res. Clin. Pract. 82 (Suppl 2),

S102-107.

4. Brand, C.L., Galsgaard, E.D., Tornehave, D., Rømer, J., Gotfredsen, C.F., Wassermann, K., Knudsen, L.B., Vølund, A., Sturis, J. 2009. Synergistic effect of the human GLP-1 analogue liraglutide and a dual PPARalpha/gamma agonist on glycaemic control in Zucker diabetic fatty rats. Diabetes Obes. Metab. 11, 795-803.

5. Burkey, B.F,. Li, X., Bolognese, L., Balkan, B., Mone, M., Russel, M., Hughes, T.E., Wang, P.R. 2005. Acute and chronic effects of the incretin enhancer vildagliptin in insulin resistant rats. J. Pharmacol. Exp. Ther. 315, 688-695.

6. Butler, A.E., Janson, J., Bonner-Weir, S., Ritzel, R., Rizza, R.A., Butler, P.C. 2003. B-Cell deficit and increased ß-cell apoptosis in humans with type 2 diabetes. Diabetes 52, 102-110.

7. Cummings, B.P., Stanhope, K.L., Graham, J.L., Baskin, D.G., Griffen, S.C., Nilsson, C., Sams, A., Knudsen, L.B., Raun, K., Havel, P.J. 2010. Chronic administration of the glucagon-like peptide-1 analog, liraglutide, delays the onset of diabetes and lowers triglycerides in UCD-T2DM rats. Diabetes 59, 2653-2661.

8. Dunning, B.E., Foley, J.E., Ahrén, B. 2005. Alpha cell function in health and disease: influence of glucagon-like peptide-1. Diabetologia 48, 1700-1713.

9. Dunning, B.E., Gerich, J.E. 2007. The role of alpha-cell dysregulation in fasting and postprandial hyperglycemia in type 2 diabetes and therapeutic implications. Endocr. Rev. 28, 253-283.

10. Duttaroy, A., Voelker, F., Merriam, K., Zhang, X., Ren, X., Subramanian, K., Hughes, T.E., Burkey, B.F. 2011. The DPP-4 inhibitor vildagliptin increases pancreatic beta cell mass in neonatal rats. Eur. J. Pharmacol. 650, 703-707.

11. Ehses, J.A., Lacraz, G., Giroix, M.H., Schmidlin, F., Coulaud, J., Kassis, N., Irminger, J.C., Kergoat, M., Portha, B., Homo-Delarche, F., Donath, M.Y. 2009. IL-1 antagonism reduces hyperglycemia and tissue inflammation in the type 2 diabetic GK rat. Proc. Natl. Acad. Sci. USA 106, 13998-14003.

12. Ellingsgaard, H., Hauselmann, I., Schuler, B., Habib, A.M., Baggio, L.L., Meier, D.T., Eppler, E., Bouzakri, K., Wueest, S., Muller, Y.D., Hansen, A.M.K., Reinecke, M., Konrad, D., Gassmann, M., Reimann, F., Halban, P.A., Gromada, J., Drucker, D.J., Gribble, F.M., Ehses, J.A., Donath, M.Y. 2011. Interleukin-6 enhances insulin secretion by increasing glucagon-like peptide-1 secretion from L cells and alpha cells. Nat. Med. 17, 1481-1489.

13. Funakoshi, S,. Fujimoto, S., Hamasaki, A., Fujiwara, H., Fujita, Y., Ikeda, K., Hamamoto, Y., Hosokawa, M., Seino, Y., Inagaki, N. 2008. Analysis of factors influencing pancreatic beta-cell function in Japanese patients with type 2 diabetes: association with body mass index and duration of diabetic exposure. Diabetes Res. Clin. Pract. 82, 353-358.

14. Goto, Y., Suzuki, K., Ono, T., Sasaki, M., Toyota, T. 1988. Development of diabetes in the non-obese NIDDM rat (GK rat). Adv. Exp. Med. Biol. 246, 29-31.

15. Gromada, J., Franklin, I., Wollheim, C.B. 2007. Alpha-cells of the endocrine pancreas: 35 years of research but the enigma remains. Endocr. Rev. 28, 84-116.

16. Hare, K.J., Vilsbøll, T., Asmar, M., Deacon, C.F., Knop, F.K., Holst, J.J. 2010. The glucagonostatic and insulinotropic effects of glucagon-like peptide 1 contribute equally to its glucose-lowering action. Diabetes 59, 1765-1770.

17. Higa, M., Zhou, Y.T., Ravazzola, M., Baetens, D., Orci, L., Unger, R.H. 1999. Troglitazone prevents mitochondrial alterations, beta cell destruction, and diabetes in obese prediabetic rats. Proc. Nat.l Acad. Sci. U S A 96, 11513-11518.

18. Homo-Delarche, F., Calderari, S., Irminger, J.C., Gangnerau, M.N., Coulaud, J., Rickenbach, K., Dolz, M., Halban, P., Portha, B., Serradas, P. 2006. Islet inflammation and fibrosis in a spontaneous model of type 2 diabetes, the GK rat. Diabetes 55, 1625-1633.

19. Kawamori, D., Akiyama, M., Hu, J., Hambro, B., Kulkarni, R.N. 2011. Growth factor signalling in the regulation of α-cell fate. Diabetes Obes. Metab. 13 (Suppl. 1), 21-30.

20. Kodera, R., Shikata, K., Kataoka, H.U., Takatsuka, T., Miyamoto, S., Sasaki, M.,

Kajitani, N., Nishishita, S., Sarai, K., Hirota, D., Sato, C., Ogawa, D., Makino, H. 2011. Glucagon-like peptide-1 receptor agonist ameliorates renal injury through its anti-inflammatory action without lowering blood glucose level in a rat model of type 1 diabetes. Diabetologia 54, 965-978.

21. Koyama, M., Wada, R., Mizukami, H., Sakuraba, H., Odaka, H., Ikeda, H., Yagihashi, S. 2000. Inhibition of progressive reduction of islet beta-cell mass in spontaneously diabetic Goto-Kakizaki rats by alpha-glucosidase inhibitor. Metabolism 49, 347-352.

22. Koyama, M., Wada, R., Sakuraba, H., Mizukami, H., Yagihashi, S. 1998. Accelerated loss of islet beta cells in sucrose-fed Goto-Kakizaki rats, a genetic model of non-insulin-dependent diabetes mellitus. Am. J. Pathol. 153, 537-545.

23. Kwon, G., Marshall, C.A., Pappan, K.L., Remedi, M.S., McDaniel, M.L. 2004. Signaling elements involved in the metabolic regulation of mTOR by nutrients, incretins, and growth factors in islets. Diabetes 53 (Suppl 3), S225-232.

24. Lamont, B.J., Drucker, D.J. 2008. Differential antidiabetic efficacy of incretin agonists versus DPP-4 inhibition in high fat fed mice. Diabetes 57, 190-198.

25. Leiter, E.H., Gapp, D.A., Eppig, J.J., Coleman, D.L. 1979. Ultrastructural and morphometric studies of delta cells in pancreatic islets from C57BL/Ks diabetes mice. Diabetologia 17, 297-309.

26. Liu L.L., Yi, J.P., Beyer, J., Mayer-Davis, E.J., Dolan, L.M., Dabelea, D.M., Lawrence, J.M., Rodriguez, B.L., Marcovina, S.M., Waitzfelder, B.E., Fujimoto, W.Y. SEARCH for Diabetes in Youth Study Group. 2009. Type 1 and type 2 diabetes in Asian and Pacific islander U.S. youth: the SEARCH for diabetes in youth study. Diabetes Care 32 (Suppl 2), S133-140.

27. Martinez, S.C., Tanabe, K., Cras-Meneur, C., Abumrad, N.A., Bernal-Mizrachi, E., Permutt, M.A. 2008. Inhibition of FoxO1 protects pancreatic islet ß-cells against fatty acid and endoplasmic reticulum stress-induced apoptosis. Diabetes 57, 845-859.

28. Matveyenko, A.V., Dry, S., Cox, H.I., Moshtaghian, A., Gurlo, T., Galasso, R., Butler, A.E., Butler, P.C. 2009. Beneficial endocrine but adverse exocrine effects of sitagliptin in the human islet amyloid polypeptide transgenic rat model of type 2 diabetes: interactions with metformin. Diabetes 58, 1604-1615.

29. Mizukami, H., Inaba, W., Takahashi, K., Inoue, K., Sawanobori, K., Yagihashi, S. 2012. Augmented reduction of islet ß-cell mass in Goto-Kakizaki rats fed high-fat diet and its suppression by pitavastatin treatment. J. Diabetes Invest. 3, 235-244.

30. Moritoh, Y., Takeuchi, K., Hazama, M. 2010. Combination treatment with alogliptin and voglibose increases active GLP-1 circulation, prevents the development of diabetes and preserves pancreatic beta-cells in prediabetic db/db mice. Diabetes Obes. Metab. 12, 224-233.

31. Mu, J., Woods, J., Zhou, Y.P., Roy, R.S., Li, Z., Zycband, E., Feng, Y., Zhu, L., Li, C., Howard, A.D., Moller, D.E., Thornberry, N.A., Zhang, B.B. 2006. Chronic inhibition of dipeptidyl peptidase-4 with a sitagliptin analog preserves pancreatic beta-cell mass and function in a rodent model of type 2 diabetes. Diabetes 55, 1695-1704.

32. Mukai, E., Fujimoto, S., Sato, H., Oneyama, C., Kominato, R., Sato, Y., Sasaki, M., Nishi, Y., Okada, M., Inagaki, N. 2011. Exendin-4 suppresses Src activation and reactive oxygen species production in diabetic Goto-Kakizaki rat islets in an Epac-dependent manner. Diabetes 60, 218-226.

33. Nauck, M.A., Vilsbøll, T., Gallwitz, B., Garber, A., Madsbad, S. 2009. Incretin-based therapies: viewpoints on the way to consensus. Diabetes Care 32 (Suppl 2), S223-231.

34. Paris, M., Tourrel-Cuzin, C., Plachot, C., Ktorza, A. 2004. Pancreatic ß-cell neogenesis revisited. Exp Diabetes Res 5, 111-121.

35. Portha, B., Serradas, P., Bailbé, D., Suzuki, K., Goto, Y., Giroix, M.H. 1991. Beta-cell insensitivity to glucose in the GK rat, a spontaneous nonobese model for type II diabetes. Diabetes 40, 486-491.

36. Rodriguez-Diaz, R., Dando, R., Jacques-Silva, M.C., Fachado, A., Molina, J.,

Abdulreda, M.H., Ricordi, C., Roper, S.D., Berggren, P.O., Caicedo, A. 2011. Alpha cells secrete acetylcholine as a non-neuronal paracrine signal priming beta cell function in humans. Nat. Med. 17, 888-892.

37. Sakuraba, H., Mizukami, H., Yagihashi, N., Wada, R., Hanyu, C., Yagihashi, S. 2002. Reduced beta-cell mass and expression of oxidative stress-related DNA damage in the islet of Japanese Type II diabetic patients. Diabetologia 45, 85-96.

38. Simonsen, L., Pilgaard, S., Orskov, C., Hartman, B., Holst, J.J., Deacon, C.F. 2009. Long-term exendin-4 treatment delays natural deterioration of glycaemic control in diabetic Goto-Kakizaki rats. Diabetes Obes. Metab. 11, 884-890.

39. Sudre, B., Broqua, P., White, R.B., Ashworth, D., Evans, D.M., Haigh, R., Junien, J.L., Aubert, M.L. 2002. Chronic inhibition of circulating dipeptidyl peptidase IV by FE 999011 delays the occurrence of diabetes in male Zucker diabetic fatty rats. Diabetes 51, 1461-1469.

40. Svensson, A.M., Ostenson, C.G., Efendic, S., Jansson, L. 2007. Effects of glucagon-like peptide-1-(7-36)-amide on pancreatic islet and intestinal blood perfusion in Wistar rats and diabetic GK rats. Clin. Sci. (Lond) 112, 345-351.

41. Takeda, Y., Fujita, Y., Honjo, J., Yanagimachi, T., Sakagami, H., Takiyama, Y., Makino, Y., Abiko, A., Kieffer, T.J., Haneda, M. 2012. Reduction of both beta cell death and alpha cell proliferation by dipeptidyl peptidase-4 inhibition in a streptozotocin-induced model of diabetes in mice. Diabetologia 55, 404-412.

42. Tourrel, C., Bailbe, D., Lacorne, M., Meile, M.J., Kergoat, M., Portha, B. 2002. Persistent improvement of type 2 diabetes in the Goto-Kakizaki rat model by expansion of the ß-cell mass during the prediabetic period with glucagon-like peptide-1 or exendin-4. Diabetes 51, 1443-1452.

Figure legends

Fig. 1. Effects of vildagliptin on blood glucose concentrations during a 2 g/kg oral glucose tolerance test. GK rats show marked hyperglycemia after the glucose challenge. Vildagliptin treatment significantly suppressed the post-challenge increases in blood

glucose concentrations at weeks 8 and 18 of treatment. Vildagliptin did not significantly affect blood glucose concentrations in Wistar rats. Open squares, Wistar rats; closed square, vildagliptin-treated Wistar rats; open circles, GK rats; closed circles, vildagliptin-treated GK rats. *P < 0.01 vs Wistar rats and vildagliptin-treated Wistar rats; †P < 0.01 vs untreated GK rats; ‡P < 0.05 vs untreated GK rats.

Fig. 2. Effects of vildagliptin on insulin secretion after a glucose challenge, plasma glucagon and GLP-1 concentrations, and pancreatic insulin content. (A) Insulin secretion at 30 min after the glucose challenge was significantly blunted in GK rats compared with Wistar rats. Vildagliptin significantly increased insulin secretion in GK rats. (B) Plasma glucagon concentrations were significantly increased in GK rats, and this was significantly reduced by vildagliptin. By contrast, plasma GLP-1 concentrations were significantly reduced in GK rats, and were restored to normal levels by vildagliptin. (C) There was a marked decrease in pancreatic insulin content in GK rats compared with Wistar rats. Vildagliptin significantly increased insulin content. Values are means ± S.E.M. W, untreated Wistar rats; W+V, vildagliptin-treated Wistar rats; GK, GK rats; GK+V, vildagliptin-treated GK rats. *P < 0.01 vs Wistar rats and vildagliptin-treated Wistar rats; †P < 0.01 vs untreated GK rats.

Fig. 3. Effects of vildagliptin on islet histology and the composition of ß and α cells. (A) In normal Wistar rats, ß cells occupied most of the central region of the islets. Vildagliptin did not affect islet architecture, although there was slight expansion of the contour. Marked loss of ß cells and distortion of islet shape with a loss of cellular polarity were evident in untreated GK rats, while vildagliptin preserved islet architecture by restoring ß cells. (B) The volume density of islet ß cells was significantly decreased in GK rats, but was restored by vildagliptin. α cell volume density was not significantly different among the four groups. Values are means ± S.E.M. W, untreated Wistar rats; W+V, vildagliptin-treated Wistar rats; GK, GK rats; GK+V, vildagliptin-treated GK rats; Vß, volume density of islet ß cells; Vα, volume density of islet α cells. *P < 0.01 vs Wistar rats and vildagliptin-treated Wistar rats; †P < 0.01 vs untreated GK rats.

Fig. 4. Effects of vildagliptin on the proliferation of islet endocrine cells. Proliferation was determined by double-labeling of Ki-67 and insulin or glucagon. (A) The proliferation of ß cells in GK rats (upper center) was not significantly different from that in Wistar rats (upper left). Vildagliptin enhanced the proliferation of α cells (upper

right). The proliferation of α cells in GK rats (lower center) was similar to that in Wistar rats (lower left). Vildagliptin enhanced α cell proliferation in GK rats (lower right). (B) Quantitative analyses confirmed that there were significant increases in Ki-67-positive ß and α cells compared with those in untreated GK rats. Values are means ± S.E.M. W, untreated Wistar rats; W+V, vildagliptin-treated Wistar rats; GK, GK rats; GK+V, vildagliptin-treated GK rats. *P < 0.01 vs untreated GK rats.

Fig. 5. Immunohistochemical expression of PDX-1 in the islet. (A) PDX-1 expression (brown) in the islets of GK rats (lower left) was markedly reduced compared with that in Wistar rats (upper left). Vildagliptin did not affect PDX-1 expression in Wistar rats (upper right), but restored PDX-1 expression in GK rats (lower right). (B) Semiquantitative analysis of PDX-1 expression confirmed these findings. Values are means ± S.E.M. W, untreated Wistar rats; W+V, vildagliptin-treated Wistar rats; GK, GK rats; GK+V, vildagliptin-treated GK rats. *P < 0.01 vs Wistar rats; †P < 0.01 vs untreated GK rats.

Fig. 6. Effects of vildagliptin on the immunohistochemical expression of p-mTOR, p-S6RP and FoxO1 in islets. (A) Islet p-mTOR expression (brown), a cell signal for proliferation, was apparently reduced in GK rats (upper center) compared with Wistar rats (upper left). Islet p-mTOR expression was restored to near normal levels in vildagliptin-treated GK rats (upper right). Similarly, p-S6RP expression (blue with a red background corresponding to insulin) was reduced in GK rats (middle center) compared with Wistar rats (middle left). Vildagliptin restored islet p-S6RP expression in GK rats (middle right). Unlike the proliferation signals, the islet expression of FoxO1, which is associated with apoptosis (brown with a red background corresponding to glucagon) was enhanced in GK rats (lower center) compared with Wistar rats (lower left). The expression of FoxO1 was suppressed in vildagliptin-treated GK rats (lower right). (B) Semiquantitative analysis confirmed these findings. Values are means ± S.E.M. W, untreated Wistar rats; W+V, vildagliptin-treated Wistar rats; GK, GK rats; GK+V, vildagliptin-treated GK rats. *P < 0.01 vs Wistar rats; †P < 0.01 vs untreated GK rats; ‡P < 0.05 vs untreated GK rats.

Fig. 7. Effects of vildagliptin on oxidative stress-related cell damage evaluated by 8-hydroxy-2'-deoxyguanosine (8OHdG) staining in the islet. (A) Islets of untreated GK rats showed abundant 8OHdG staining (lower left), while Wistar rats yielded only faint staining (upper left). Vildagliptin did not affect 8OHdG staining in Wistar rats (upper

right), but significantly reduced the level of staining in GK rats (lower right). (B) Quantitative analysis confirmed that 8OHdG staining was significantly increased in untreated GK rats and was suppressed by vildagliptin treatment. Values are mean ± S.E.M. W, untreated Wistar rats; W+V, vildagliptin-treated Wistar rats; GK, GK rats; GK+V, vildagliptin-treated GK rats. *P < 0.01 vs Wistar rats; †P < 0.05 vs untreated GK rats.

Fig. 8. Vildagliptin increased the number of small neogenetic islets identified by insulin and glucagon immunostaining. (A) Isolated small neogenetic islets composed of <4 ß cells were commonly seen in the ductal (upper left), periductal (upper center), and acinar (upper right) areas in GK rats. Small islets composed of α cells were also common in these rats. (B) Vildagliptin significantly increased the number of neogenetic islets composed of either ß or α cells in GK rats, but not in Wistar rats. The small neogenetic islet composed of ß and α cells was most common in the acinar area, although there was no site preference of newly derived islets in the vildagliptin-treated group. Values are means ± S.E.M. *P < 0.01 vs untreated GK rats; †P < 0.01 vs Wistar rats; ‡P < 0.05 vs Wistar rats; **P < 0.05 vs untreated GK rats.

Fig. 9. Effects of vildagliptin on macrophage infiltration in islets. (A) Macrophage infiltration is a characteristic of GK rats (lower left). Vildagliptin inhibited macrophage infiltration in GK rats (lower right). (B) Quantitative analysis confirmed that macrophage infiltration was greater in GK rats than in Wistar rats. Vildagliptin significantly reduced macrophage infiltration. Values are means ± S.E.M. W, untreated Wistar rats; W+V, vildagliptin-treated Wistar rats; GK, GK rats; GK+V, vildagliptin-treated GK rats. *P < 0.01 vs untreated GK rats; †P < 0.01 vs untreated GK rats.

Legend for Appendix A. Supplementary information

Absence of apoptotic cells in the islet of GK rats. In contrast to the clear presence of apoptotic cells (arrows) positive for TUNEL in the lymphoid tissues adjacent to exocrine pancreas, there is no positive cell in the islet in Wistar and GK rats either treated with or without vildagliptin on the same slide with the identical staining conditions. There are infrequenly positive acinar cells in both Wistar and GK rats. GK rats showed hemosiderin deposition in the pancreas.

Appendix A. Supplementary information

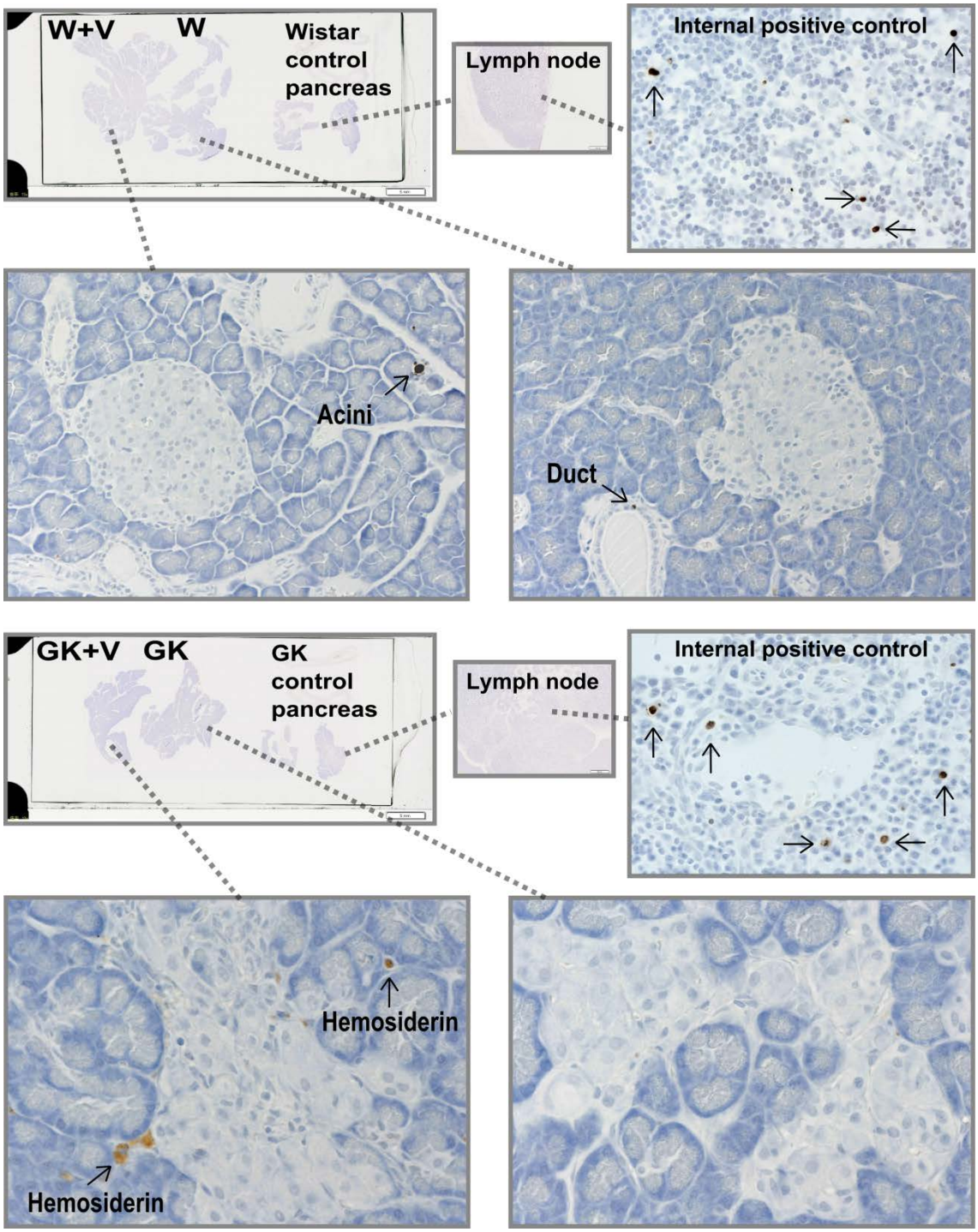

Fig.1

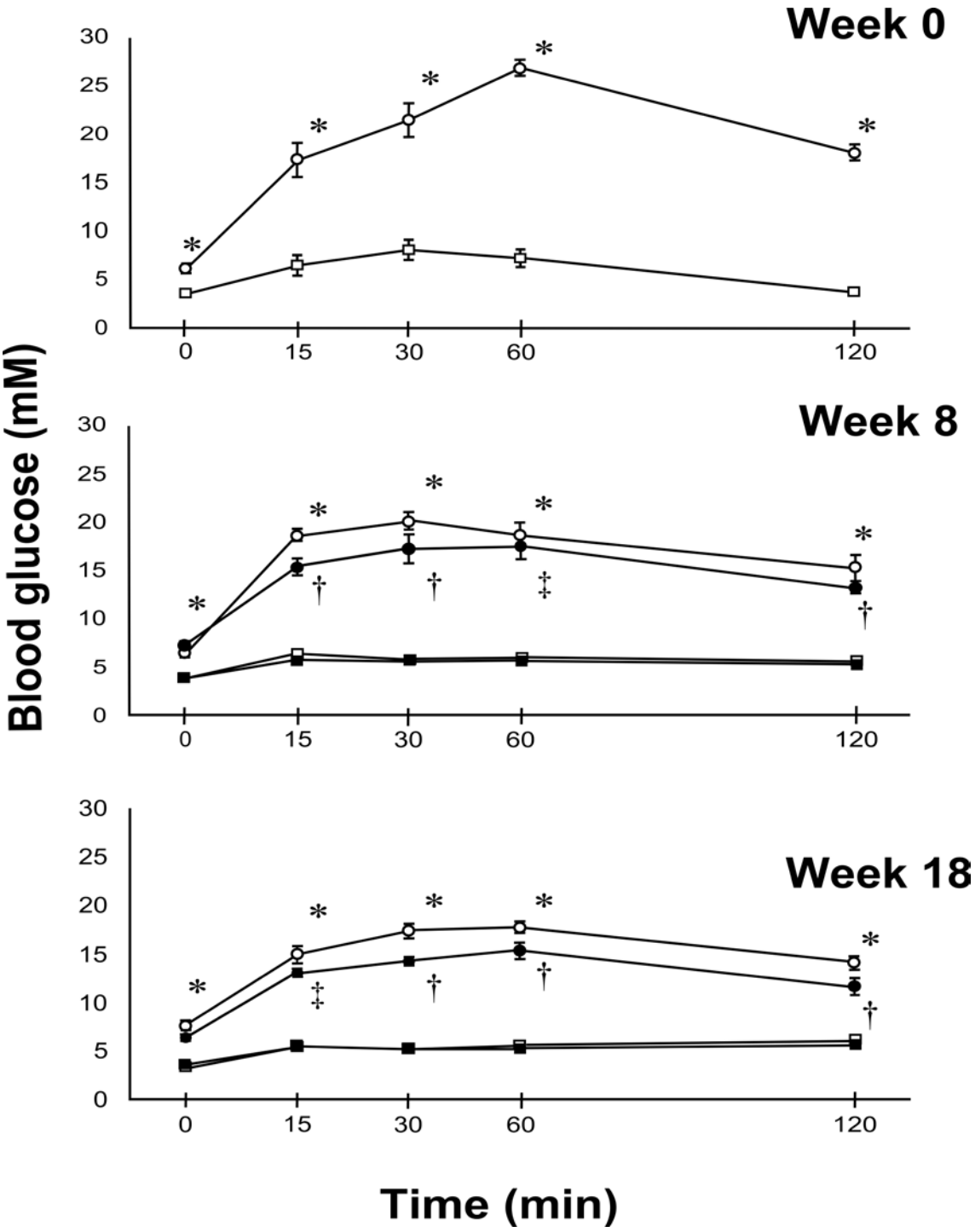
Week 0
Week 8
Week 18
Blood glucose (mM)
Time (min)
0
5
10
15
20
25
30
0
15
30
60
120

Fig.2

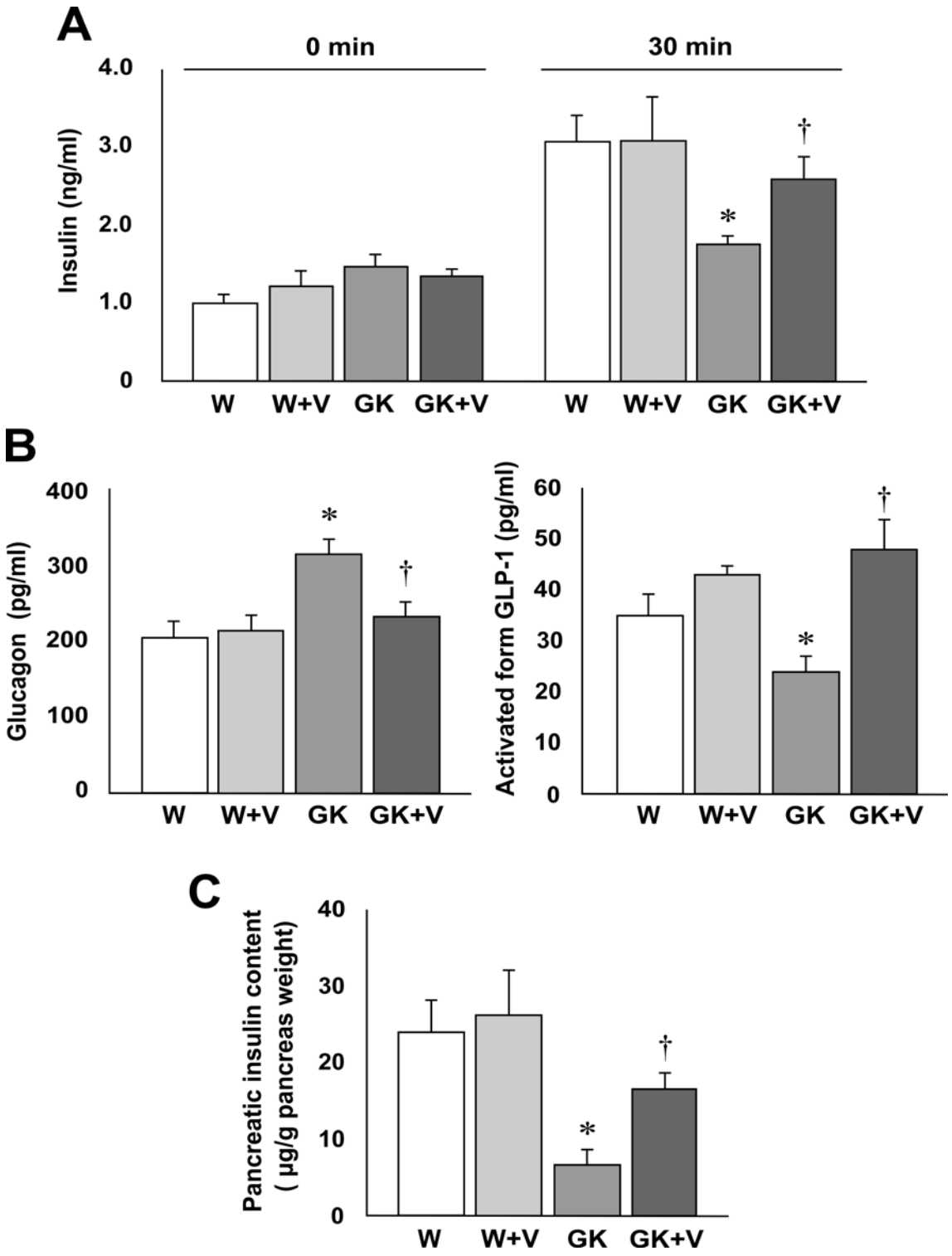
A
0 min
30 min
Insulin (ng/ml)
4.0
3.0
2.0
1.0
0
W
W+V
GK
GK+V
*
†
B
Glucagon (pg/ml)
400
300
200
100
0
Activated form GLP-1 (pg/ml)
60
50
40
30
20
10
C
Pancreatic insulin content
(μg/g pancreas weight)
40
30
20
10

Fig.3

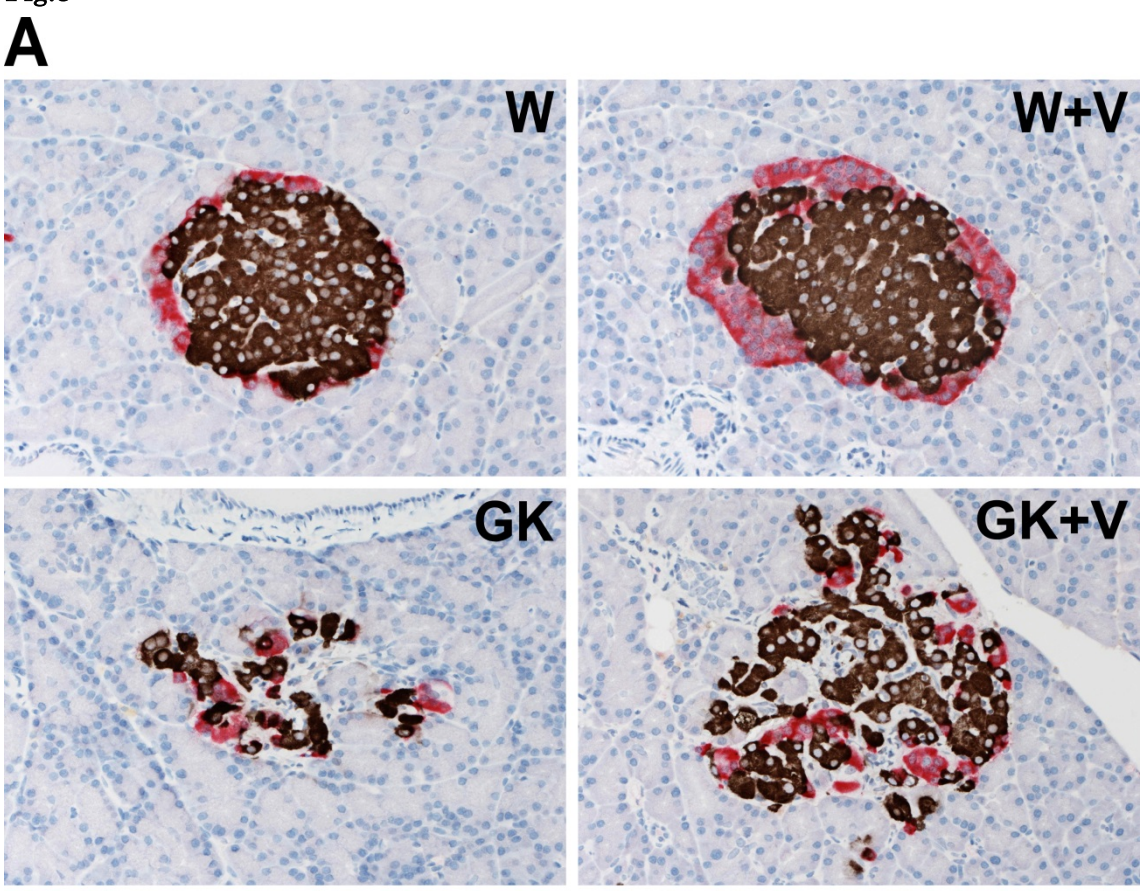

Fig.4

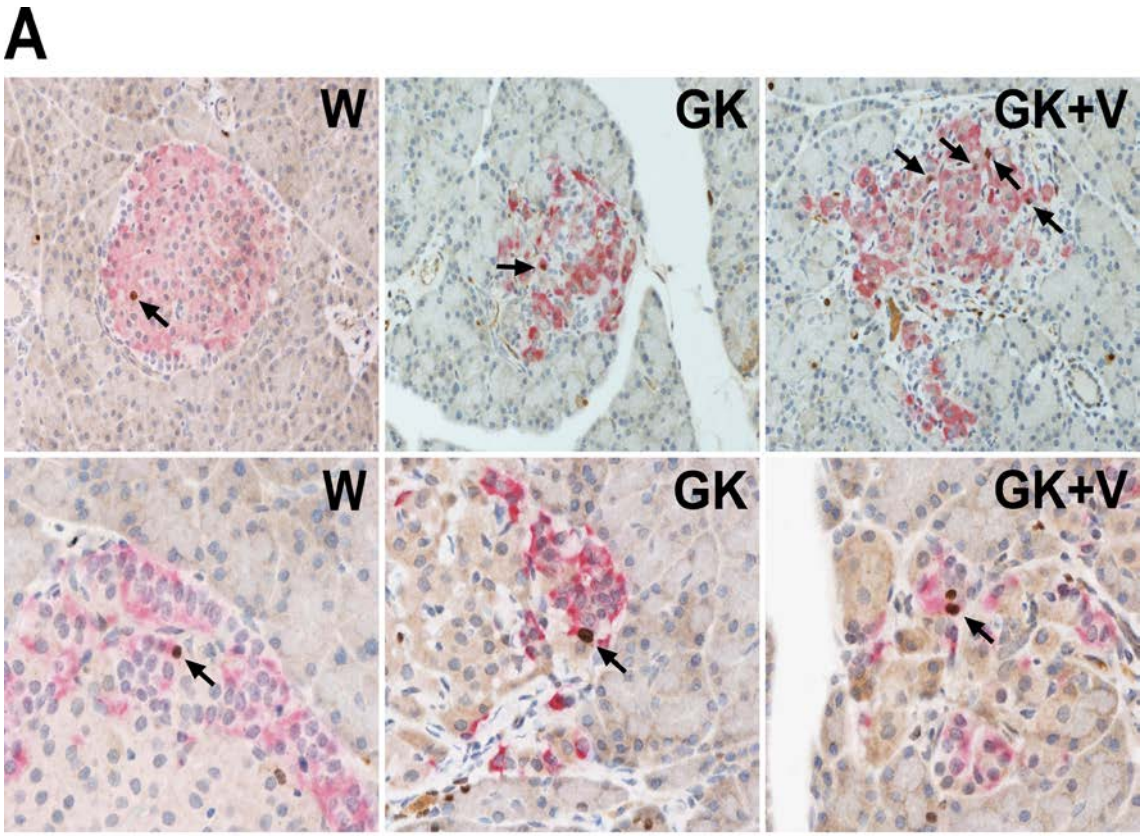
A
W
GK
GK+V
W
GK
GK+V

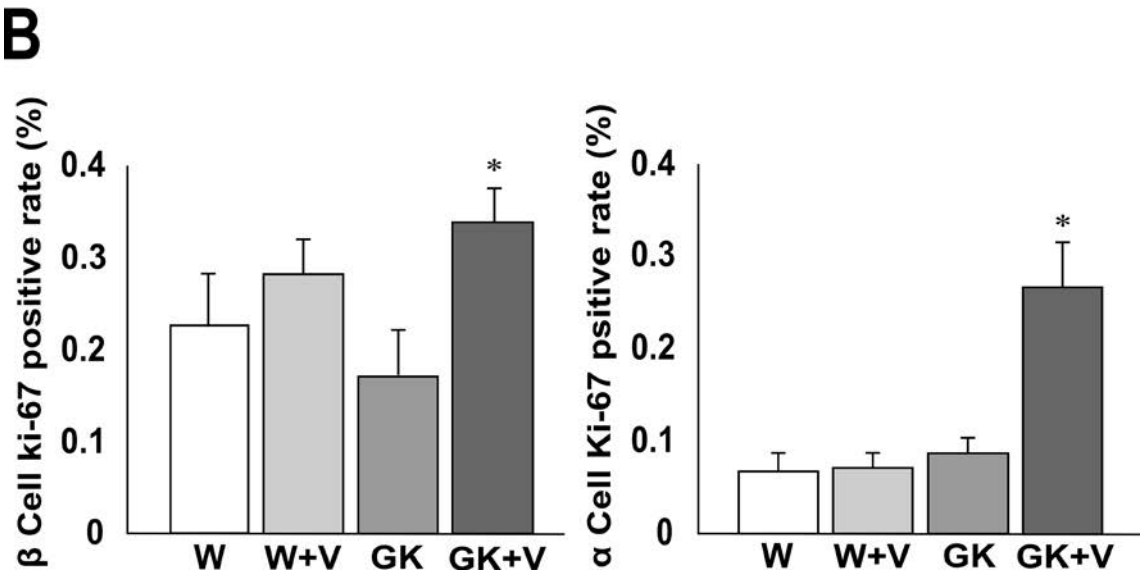
B
β Cell ki-67 positive rate (%)
0.4
0.3
0.2
0.1
0
*
W
W+V
GK
GK+V
α Cell Ki-67 psitive rate (%)
0.4
0.3
0.2
0.1
0
*
W
W+V
GK
GK+V

Fig.5

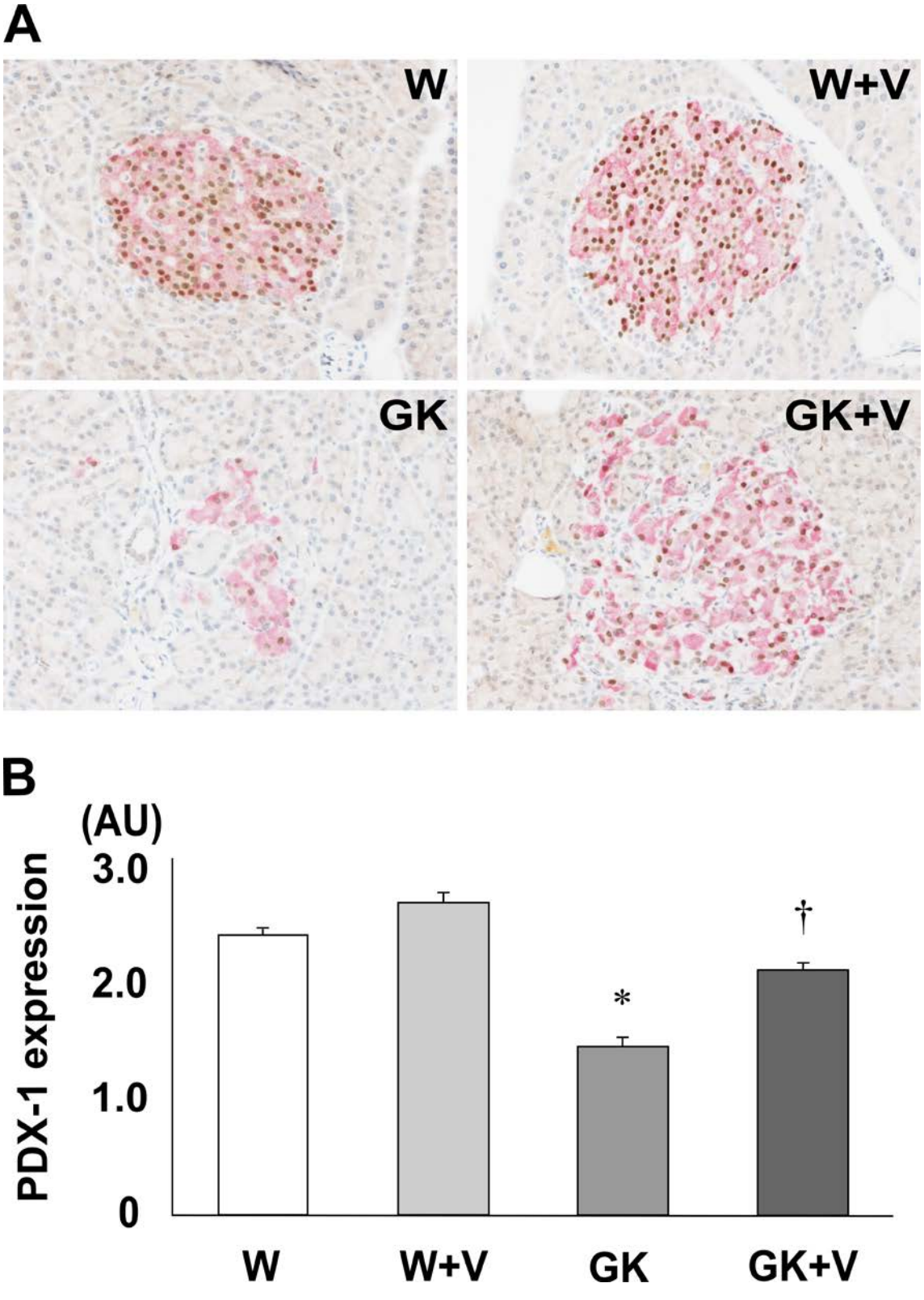

Fig.6

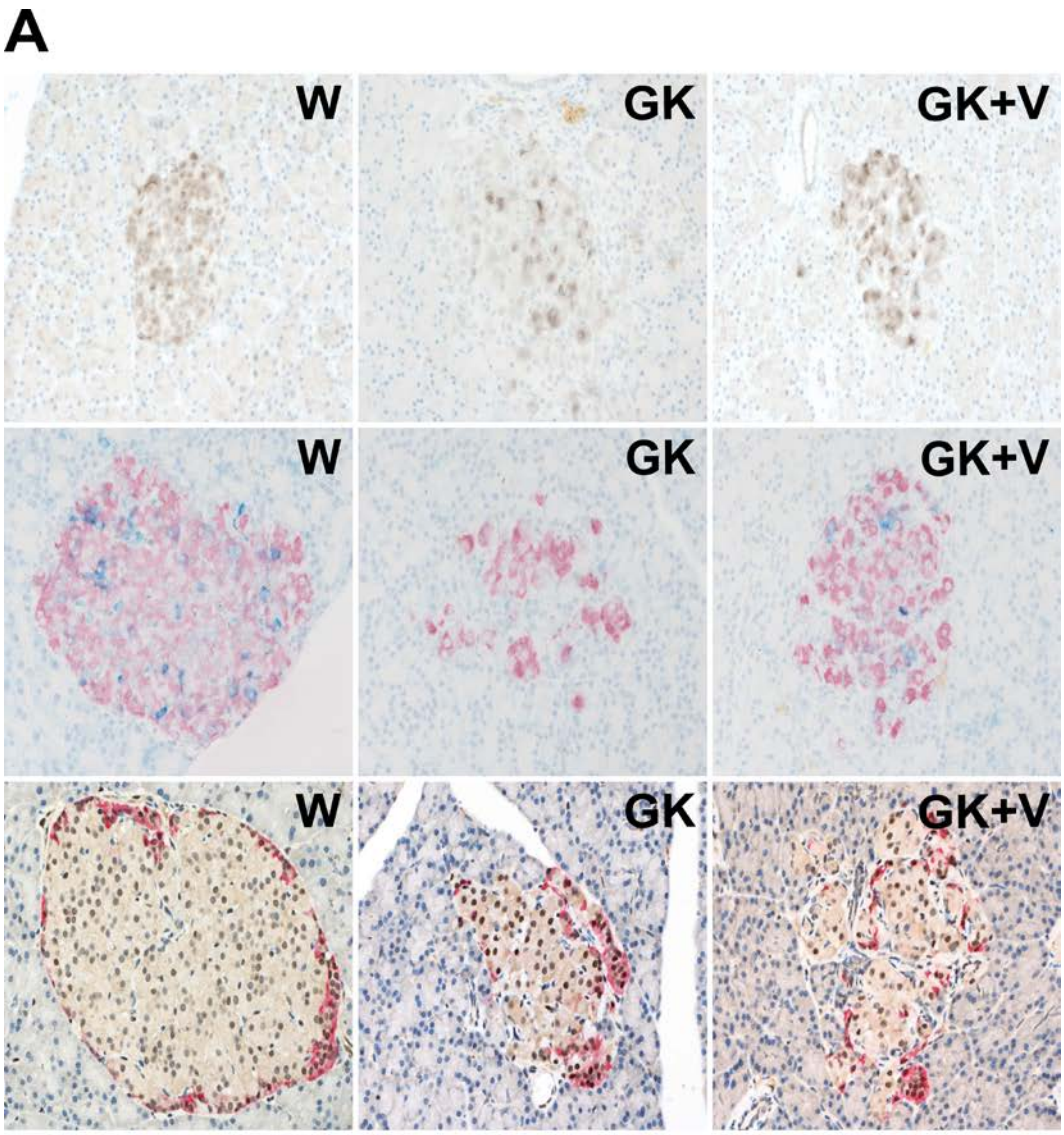
A
W
GK
GK+V
W
GK
GK+V
W
GK
GK+V

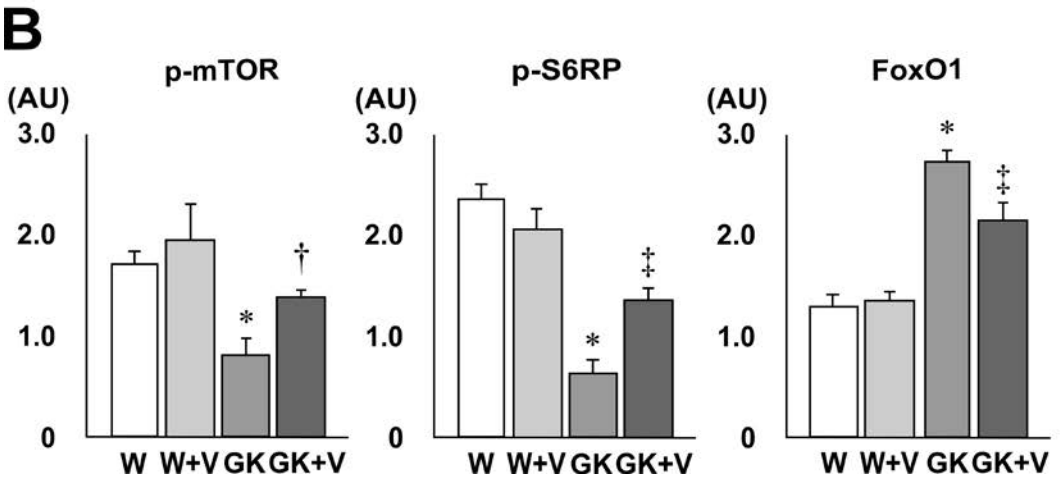
B
p-mTOR
(AU)
3.0
2.0
1.0
0
W W+V GK GK+V
p-S6RP
(AU)
3.0
2.0
1.0
0
W W+V GK GK+V
FoxO1
(AU)
3.0
2.0
1.0
0
W W+V GK GK+V

Fig.7

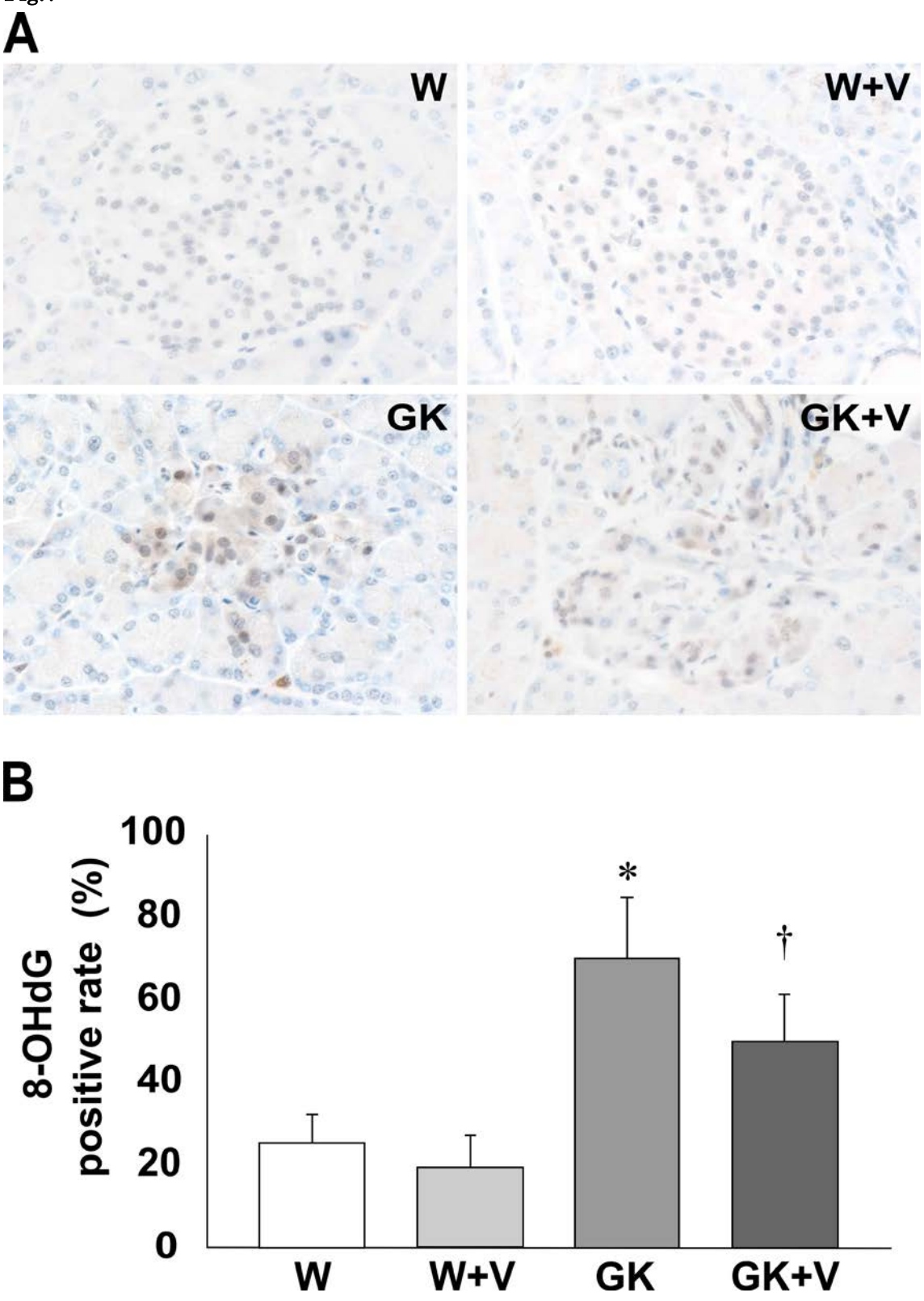

Fig.8

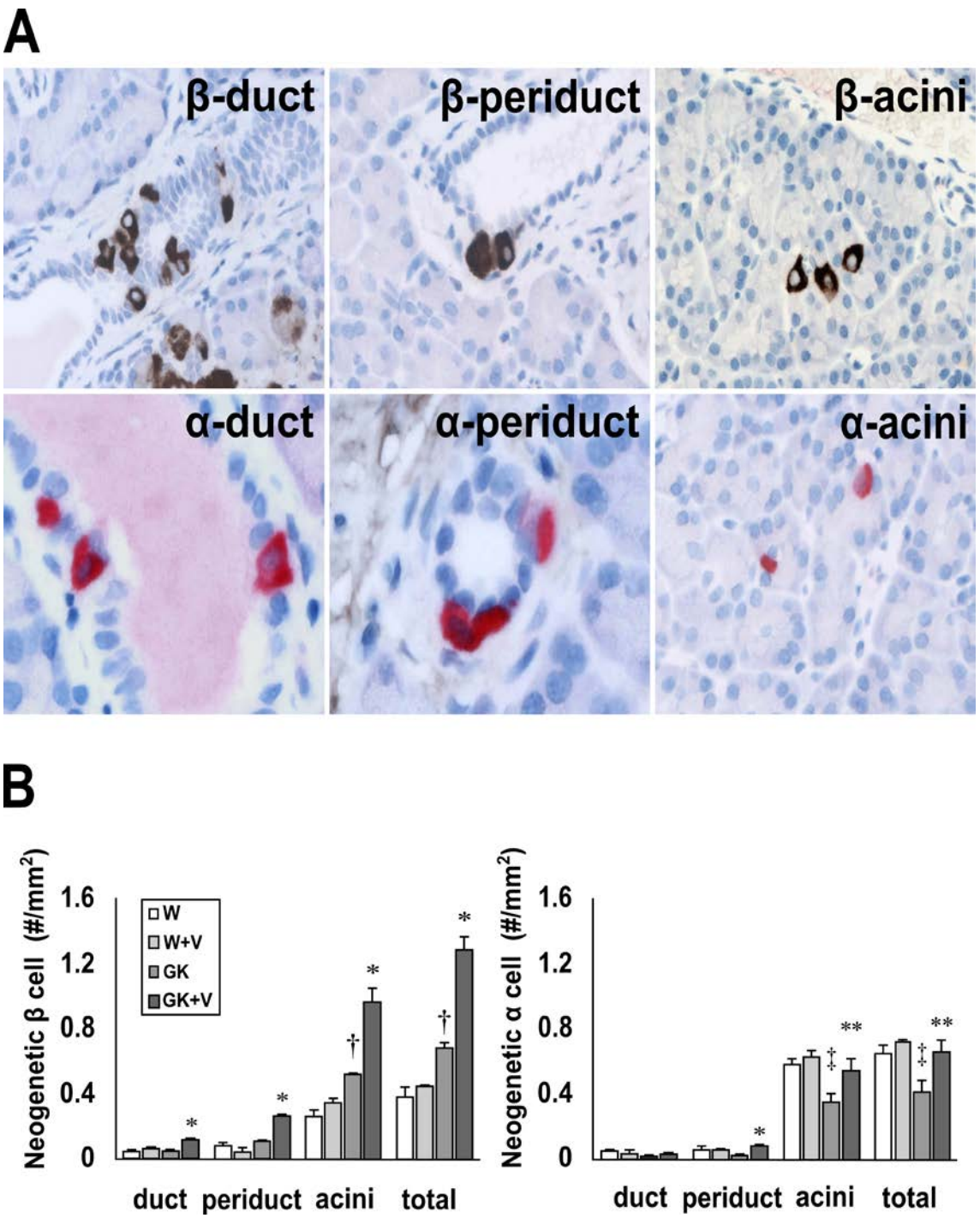
A
β-duct
β-periduct
β-acini
α-duct
α-periduct
α-acini
B
Neogenetic β cell (#/mm²)
1.6
1.2
0.8
0.4
0
W
W+V
GK
GK+V
duct
periduct
acini
total
Neogenetic α cell (#/mm²)

Fig.9

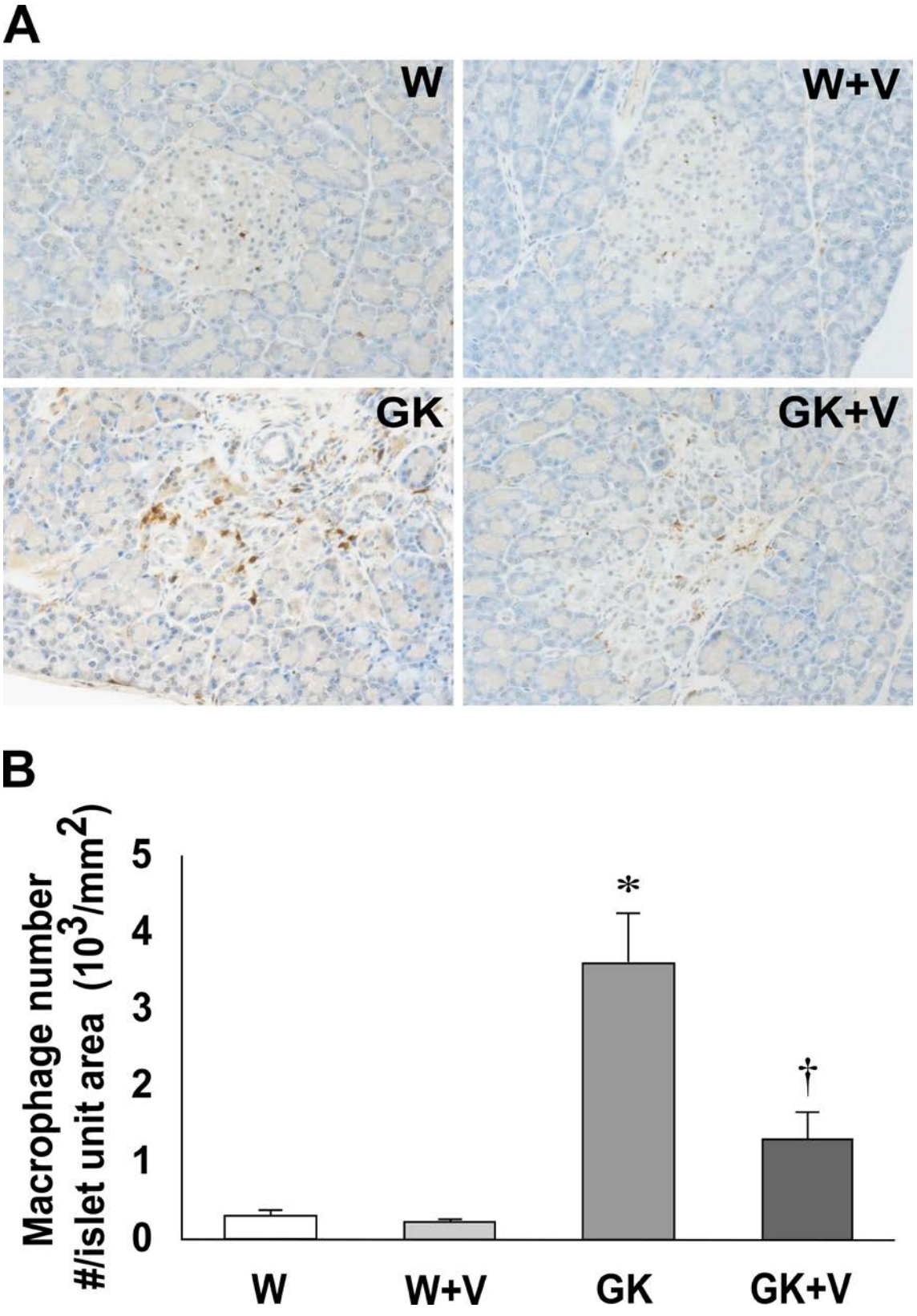
A
W
W+V
GK
GK+V
B
Macrophage number
#/islet unit area (10^3/mm^2)
0
1
2
3
4
5
*
†
W
W+V
GK
GK+V